Submitted, accepted and published by
Applied Energy, 2015, 157, 462-474

Conceptual design of a 100 MW_{th} CLC unit for solid fuel combustion

Alberto ABAD[1]*, Juan ADÁNEZ[1], Pilar GAYÁN[1], Luis F. de DIEGO[1], Francisco GARCÍA-LABIANO[1], Gerald SPRACHMANN[2]

[1] *Instituto de Carboquímica (ICB-CSIC), Miguel Luesma Castán 4, E-50018 Zaragoza, Spain*

[2] *Shell Global Solutions International BV. Amsterdam, The Netherlands*

**Corresponding Author, abad@icb.csic.es*

Abstract

The conceptual design of a 100 MW_{th} unit for coal combustion with CO_2 capture by *in-situ* Gasification Chemical Looping Combustion (*i*G-CLC) was done. Ilmenite was considered the oxygen carrier and a highly reactive sub-bituminous coal was the fuel. The main components of the *i*G-CLC unit were a fuel reactor, a carbon stripper and an air reactor. Mass and enthalpy balances were performed to determine the solids circulation flow rate**,** temperature of the reactors, steam and air requirements, and heat duty of heat exchangers. Fluid dynamics considerations and cyclones sizes were taken into account for the conceptual design and the dimensioning of these devices. In addition, optimized operating conditions obtained with a mathematical model were considered in the design procedure. Then, the performance of the *i*G-CLC unit was estimated with the model. Some benefits were identified when recirculated CO_2 was used to fluidize the carbon stripper and fuel reactor, regarding both fuel reactor performance and energy integration of the *i*G-CLC system. Thus, a CO_2 capture value of 95% with a carbon stripper with 98% efficiency and an oxygen demand in exit gases from the fuel reactor of 7% was predicted with a solids inventory in the fuel reactor of 750 kg/MW_{th}. Moreover, the energy penalty related to steam generation was minimized when H_2O was replaced by CO_2. Results presented in this work can be used to estimate the net efficiency of the plant in future works.

Submitted, accepted and published by
Applied Energy, 2015, 157, 462-474

Keywords: CO_2 capture; Chemical Looping Combustion; *i*G-CLC; Coal; Design; Modelling.

1 Introduction

Chemical Looping Combustion (CLC) has been developed over the past few decades as an efficient way to capture the CO_2 from combustion processes burning fossil fuels. When a solid fuel, e.g. coal, is used as fuel the process is known as *in-situ* Gasification Chemical Looping Combustion (*i*G-CLC). The reactor scheme for the *i*G-CLC process is shown in Figure 1. It consists of two reactors, the fuel and air reactors. A solid oxygen carrier circulates continuously between them [1].

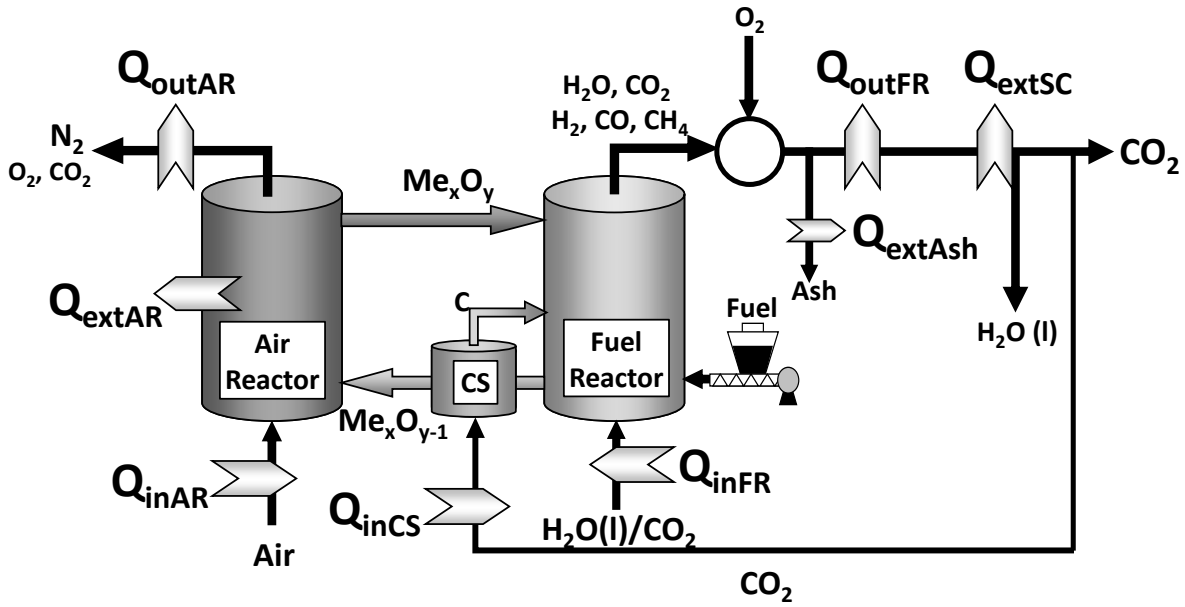

Figure 1. Reactor scheme of the *i*G-CLC process with solid fuels, including enthalpy fluxes.

The solid fuel is fed into the fuel reactor, where is physically mixed with the oxygen carrier and coal devolatilization happens according reaction (1) followed by *in-situ* gasification by H_2O and CO_2; reactions (2-3). Thus, the fuel reactor is fluidized by H_2O and/or CO_2, which acts also as a gasification agent. Then, the resulting gases are oxidized through reduction of the oxidized form of the oxygen carrier, Me_xO_y, by means of reaction (4). The water-gas shift

(WGS) equilibrium can also be relevant in the fuel reactor; reaction (5). The oxygen carrier, reduced in the fuel reactor to Me_xO_{y-1}, is transferred to the air reactor where reaction (6) takes place with oxygen from air. Thus the oxygen carrier is regenerated to start a new cycle. Ideally, the stream of combustion gases from the fuel reactor contains primarily CO_2 and H_2O, but unburnt compounds often appear in *i*G-CLC [2], mostly CO, H_2, CH_4 and H_2S [3], in contrast to what happens in the Chemical Looping with Oxygen Uncoupling (CLOU) process [4]. An oxygen polishing step may be necessary for complete combustion to CO_2 and H_2O [5]. After that, highly concentrated CO_2, ready for compression and sequestration, is obtained by condensing steam.

$$\text{Solid fuel} \rightarrow H_2O + \text{Volatile matter} + \text{Char} \quad (1)$$

$$\text{Char} + H_2O \rightarrow H_2 + CO + \text{ash} \quad (2)$$

$$\text{Char} + CO_2 \rightarrow 2\,CO + \text{ash} \quad (3)$$

$$H_2, CO, \text{Volatile matter} + n\,Me_xO_y \rightarrow CO_2 + H_2O + n\,Me_xO_{y-1} \quad (4)$$

$$CO + H_2O \leftrightarrow H_2 + CO_2 \quad (5)$$

$$Me_xO_{y-1} + 0.5\,O_2 \rightarrow Me_xO_y \quad (6)$$

$$\text{Char} + O_2 \rightarrow CO_2 + \text{ash} \quad (7)$$

Because of the slow gasification reaction, unconverted char particles can exit the fuel reactor with the oxygen carrier. Note that if char passes to the air reactor it is burnt there to CO_2, see reaction (7). There is not an energy penalty due to char burning in the air reactor. However, this fraction of carbon is not captured, decreasing the CO_2 capture efficiency of the *i*G-CLC system. A carbon separation system, e.g. a carbon stripper, is required to avoid char particles entering the air reactor in order to reach high values of CO_2 capture.

A low cost oxygen carrier is desirable for use with solid fuels, as a partial loss is anticipated, together with the ashes. Thus, natural minerals, e.g. ilmenite [6-11], iron ore [12,13] or calcium sulphate [14], as well as waste products [15], have been successfully tested for coal combustion in CLC units ranging from 0.5 to 3000 kW_{th}.

For the scale-up of the process, the use of two interconnected circulating fluidized bed reactors is believed to be advantageous because their compact size. Thus, several design concepts of mid- and large-sized CLC units have been presented [16-25], most of them for gaseous fuels. Fluid dynamics [16-20] or scale-up criteria [21,22] have been considered for design purposes of CLC units. Design by scale-up criteria can be suitable when experimental conditions used in the reference plant (usually of smaller size) are maintained, such as oxygen carrier material and mass to flow ratios. However, a variation from the reference conditions during the design procedure is risky, and no optimum results might be obtained. Thus, the change of the oxygen carrier material in a 140 kW_{th} CLC unit resulted in unexpected incomplete combustion [26].

A theoretical model is a powerful tool to initiate the dimensioning of the reactors reducing the risks associated to the scale-up criteria procedure. Also, estimation of the performance of the designed CLC unit is relevant to calculate the net plant efficiency. Thus, the net plant efficiency was estimated 52%, including CO_2 compression, for pressurized CLC of gaseous fuels [17,18]; and 41.6%, CO_2 compression included, for atmospheric CLC of solid fuels [24]. However, often the performance of the CLC unit itself has not been simulated, but it was taken from experimental observation from CLC unit at smaller scale. In some cases, mathematical models of the CLC reactors have been used to estimate the combustion efficiency of the CLC unit, but after the design procedure [19,22,23]. Interesting was a model used to simulate the performance of a Chemical Looping with Oxygen Uncoupling (CLOU) unit, which is a special case of CLC with coal [25]. In this work, a 500 MW_{th} CLOU unit was simulated to analyse the effect of several operating conditions on the CO_2 capture rate. However, in few cases the results obtained from a mathematical model has been used for design and optimization purposes. Thus, the scale-up from 140 kW_{th} to 10 MW_{th} CLC unit was optimized, and variation in some design parameters was recommended, e.g. the cross sectional area, the pressure drop of the reactors, or the particle size [27].

Moreover, the use of scale-up criteria from CLC units with solid fuels is not straightforward because: *i*) the fluid dynamics of the fuel reactor is not directly related to the fuel power, as it is the case for gaseous fuels; and *ii*) design conditions for experimental plants do not match with optimum conditions. Actually, these units operated with a lower solids inventory [28] than was proposed by modelling results [29,30], which resulted in a low combustion efficiency (75-85%) compared to optimized conditions (90-95%) [2,28,30].

The fuel reactor and carbon stripper have been mostly fluidized by steam in several CLC units [8-10]. Few experimental works have shown the effect of using CO_2 instead of H_2O [15,31,32], where it was concluded that the carbon stripper efficiency would have to be improved when CO_2 is used because CO_2 gasification is usually slower than steam gasification [33,34], except when biomass is the fuel [35]. A high penalty on the energetic efficiency of the overall process was estimated when H_2O is used compared to the use of CO_2 [36], but the effect of the fluidizing gas on the CLC performance was not modelled.

In this work, a conceptual design of an *i*G-CLC system is presented: coal is used as the solid fuel and ilmenite is the oxygen carrier. The main dimensions of the fuel reactor, carbon stripper and air reactor are calculated. Also, loop seals and cyclones are dimensioned in order to avoid mixing of the gas streams and separate gas from solids, respectively. Information from results obtained with a validated model [28-30] about optimum operational conditions is used to calculate basic design parameters of a 100 MW_{th} CLC unit with coal. Thus, cross sectional area and pressure drop are calculated in order to match with the required solids inventory in the fuel reactor. Then, the performance of the designed CLC unit is evaluated with the model. Moreover, the relation between fuel power and fluid dynamics is evaluated by means of calculating the gas velocity as a function of the cross sectional area and the ratio between fluidization gas flow to carbon in fuel. In this sense, a template is introduced to easily carry out the dimensioning of the main devices, i.e. fuel and air reactors. Finally, the performance of the CLC unit, when CO_2 instead H_2O is used as fluidization gas, is evaluated.

Then, results obtained with the CLC model are used to present a preliminary exergy analysis by mass and enthalpy balances. This information will be relevant in order to calculate the net plant efficiency in future works.

2 Procedure

2.1 Oxygen carrier and fuel

In this work, an activated Norwegian ilmenite was considered as the oxygen carrier material [37], with a mean particle diameter of 170 μm (+100-300 μm) and an apparent density of 3710 kg/m^3. Ilmenite is 59.9 wt.% Fe_2TiO_5 and 40.1 wt.% TiO_2 in its oxidized form. During reaction with the fuel, Fe_2TiO_5 is reduced to $FeTiO_3$. The reactivity of ilmenite particles increased with the redox cycles until an "activated" state was reached [7,38,39]. This reactivity increase was similar when ilmenite particles suffered redox cycles either in TGA [38], a batch fluidized bed [39] or a CLC unit [7]. However, the oxygen transport capacity of ilmenite decreased when particles were activated in TGA due to iron migration to the particle surface [38], but no variations in the oxygen transport capacity was observed during activation in a CLC unit [7]. Differences in the degree of oxygen carrier conversion during the redox process could explain why the behaviour observed in a continuous CLC unit was different to that in a batch mode [39]. Thus, its initial value, R_{OC} = 4%, was assumed because it was believed more suitable to describe the activation process in a CLC unit [7]. If a decrease in oxygen transport capacity happened after long-term operation, slight differences on the model predictions would be advisable, being of minor relevance for high oxygen carrier to fuel ratio values, ϕ [30].

The solid fuel was "Tremedal" coal from Teruel basin in Spain, which is a highly reactive sub-bituminous coal with a lower heating value of 21990 kJ/kg. The oxygen demanded by the

coal was Ω_{SF} = 1.82 kg of oxygen per kg of coal. The mean average particle diameter was 100 μm.

Reaction kinetics for both reduction and oxidation of activated ilmenite [37] as well as steam and CO_2 gasification of the coal char (see Annex A) has been determined by TGA experiments in a similar way that those described in [34].

2.2 Mass and enthalpy balance

Figure 1 shows a scheme of the *i*G-CLC process and the energy and mass flows considered for this design. Mass and enthalpy balances were imposed on the fuel and air reactors by taking into account for the chemical processes ocurring in each reactor. For a thermal power of 100 MW_{th}, the mass flow rate of solid fuel was 4.5 kg/s, based on the LHV. The flow of air to the air reactor, $F_{in,AR}$, allowed for an air excess of 20% with respect the stoichiometric air to burn the coal fed. At the air reactor exit, the flow of N_2, O_2 and CO_2 were calculated assuming that all carbon passed to the air reactor in char particles was burnt to CO_2.

The performance of the fuel reactor was analysed by using the CO_2 capture efficiency, η_{CC}, and the total oxygen demand, Ω_T. The CO_2 capture efficiency considers the physical removal of CO_2 that would otherwise be emitted into the atmosphere. The total oxygen demand is defined as the ratio of the oxygen required to fully oxidize the unconverted gases exiting the fuel reactor to the oxygen demanded by the fuel. A relevant operational parameter in the mass balance is the solids circulation rate between the fuel and air reactors, which depends on the variation of solids conversion, ΔX_{OC}. The solids circulation was evaluated by means of the oxygen carrier to fuel ratio, ϕ, defined as the flow of transferable oxygen in the oxygen carrier flow, assumed to be fully oxidized, divided by the oxygen required to fully convert the fuel to CO_2 and H_2O. Complete information about these definitions can be found in [2,29,31].

The balance of enthalpy flux over fuel and air reactors took into account the enthalpy of the particles, gases and fuel coming into each reactor (reactant) and the enthalpy of the particles and gases leaving the reactors (products), which can be expressed as:

$$\dot{H}_{reac} = \dot{H}_{prod} - \Delta\dot{H}_i \tag{8}$$

Pre-heating of the gas streams to the air and fuel reactors was considered, Q_{inAR} and Q_{inFR}. The carbon stripper was fluidized by recirculating a fraction of CO_2 after the post-oxidation chamber of the oxygen polishing step, which was also preheated, Q_{inCS}. Q_{outAR} and Q_{outFR} are the sensible heats that can be obtained from the outlet gas flow from the air and fuel reactors, respectively, when cooled to 25 ºC. To evaluate the fraction of heat flux recovered during steam condensation, the latent heat for steam condensation at 25 ºC was calculated, $Q_{ext,SC}$. Note that ash must be purged to avoid its accumulation in the CLC unit. A purge stream was considered to be concentrated in fly ash in order to reduce the losses of oxygen carrier. Thus, the sensible heat of the ash exiting the system, Q_{extAsh}, was also included. Finally, the enthalpy balance determines the heat flux which must be extracted from the air reactor, Q_{extAR}, to control its temperature. The fuel reactor was assumed to be adiabatic.

2.3 Mathematical model for fuel reactor, carbon stripper and air reactor of a *i*G-CLC unit

A general description of the mathematical model for the three main components in a *i*G-CLC unit is shown in Figure 2. In a previous work [29], a semi-empirical model describing the fuel reactor in the *i*G-CLC process was presented. The developed model describes the reactor fluid dynamics using semi-empirical correlations presented in [40], the reaction kinetics of the coal conversion and the reaction kinetics of the oxygen carrier with evolved gases from coal. Kinetics for activated ilmenite was determined Abad et al. [37], while kinetic determination of “Taldinsky” coal is presented in the Annex A. This model was validated against data obtained in a 100 kW_{th} unit at Chalmers University of Technology [28], with some

Submitted, accepted and published by
Applied Energy, 2015, 157, 462-474

modifications regarding the reaction pathway of CH_4 and the addition of the kinetics of the water-gas shift reaction.

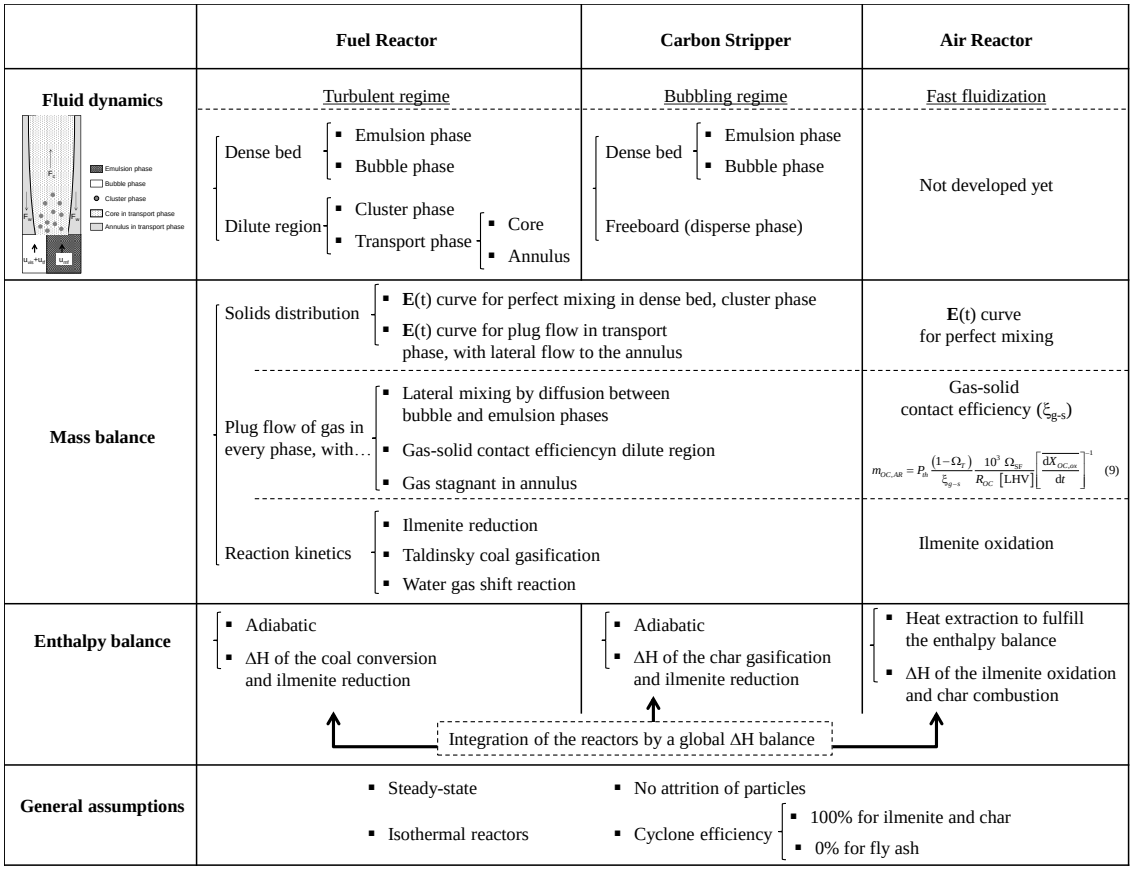

Figure 2. Main aspects included in the modelling of the main components in the 100 MW_{th} *i*G-CLC unit: fuel reactor, carbon stripper and air reactor.

A model for the carbon stripper was added by Gayán et al. [2]. The carbon stripper was a bubbling fluidized bed. Fluid dynamic was described in a previous work [41]. This model also considers kinetics of ilmenite reduction, char gasification and water gas shift reaction. The char separation efficiency was not calculated, but it was assumed.

A fluid dynamic model describing the air reactor of a *i*G-CLC unit has not been developed yet. Thus, the calculation of the solids inventory in the air reactor was based on a method presented in a previous work [37], modified to consider the efficiency in gas-solid contact, ξ_{g-s} = 0.4 [42].

Main outputs from the fuel reactor model are: *i*) solid flux to the fuel reactor cyclone; *ii*) exit gas flow and composition from air and fuel reactor; *iii*) conversion of oxygen carrier and char; *iv*) mass fraction of char in the solids in fuel reactor. From these results, the CO_2 capture efficiency, η_{CC}, and the total oxygen demand, Ω_T, were calculated to evaluate the performance of the *i*G-CLC unit. For preliminary estimations, attrition of oxygen carrier particles was not considered, as well as no solids in the exit gas stream was assumed. Thus, the total oxygen demand only considered the oxygen required for unburnt gases. More information on the reactor model is available in previous works [2,28-30].

3 Conceptual design of the 100 MW_{th} *i*G-CLC unit

The conceptual design is shown in Figures 3 and 4. It was based on two interconnected circulating fluidized bed reactors, the air and fuel reactor, and a carbon stripper, being a bubbling fluidized bed. The solid fuel is fed into the fuel reactor, which can be fluidized by H_2O, CO_2 or mixtures of them. This concept was adopted in several *i*G-CLC pilot studies [8-10], and the design includes the calculation of the solids inventory in each reactor. Mass and energy balances, fluid dynamics considerations and the performance of the fuel reactor predicted by a theoretical model previously developed, were taken into account for the *i*G-CLC system design. The nominal thermal power was 100 MW_{th} based on the lower heating value of "Tremedal" coal.

Submitted, accepted and published by
Applied Energy, 2015, 157, 462-474

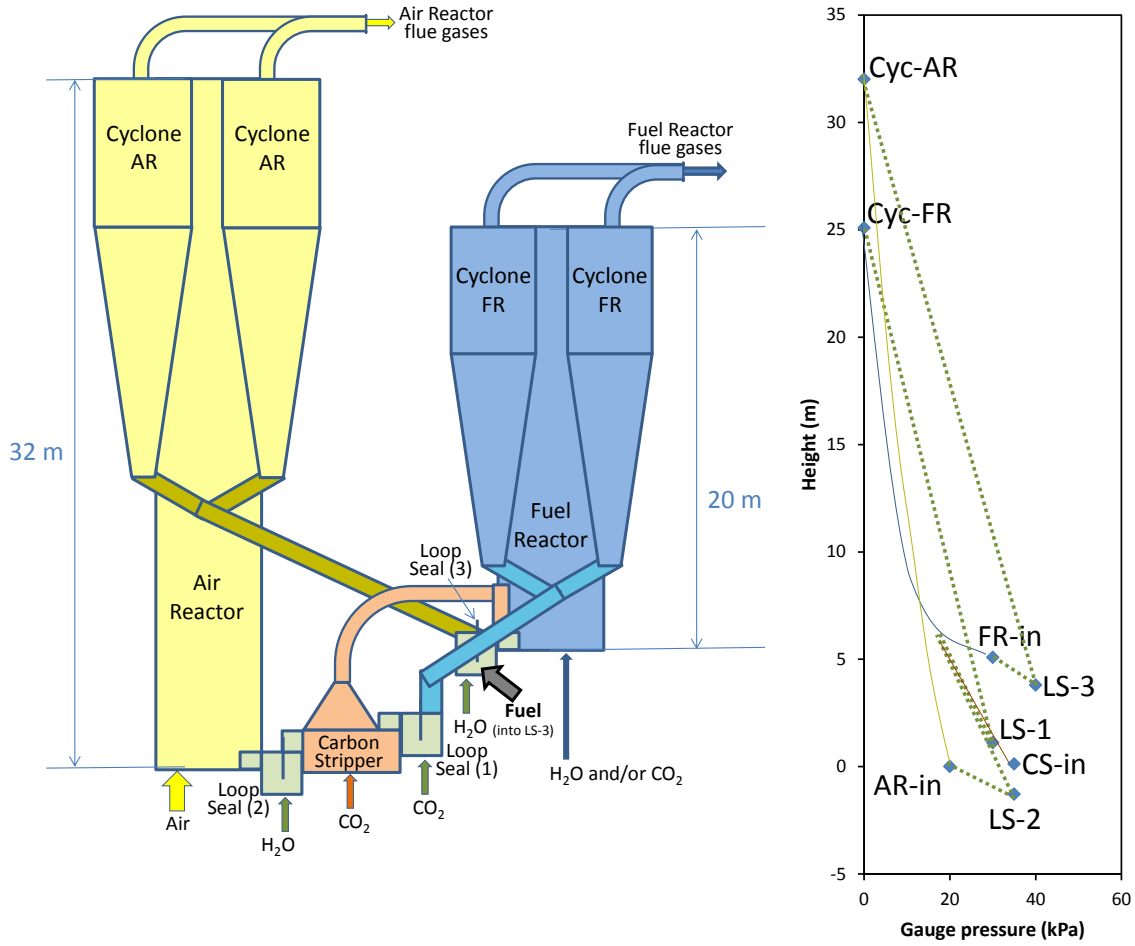

Figure 3. Elevation for the design layout of the 100 MW_{th} iG-CLC system and pressure profile.

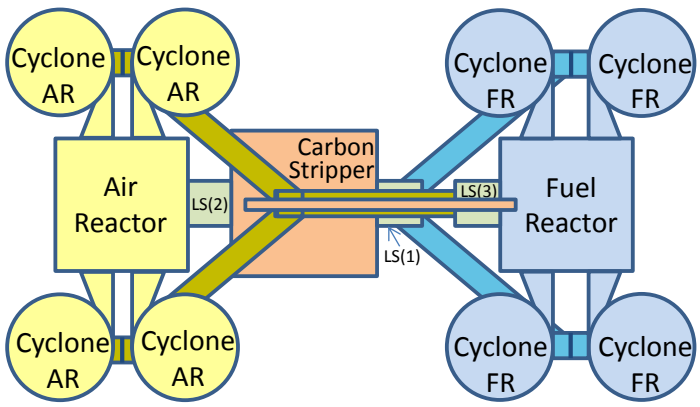

Figure 4. Plan for the design layout of the 100 MW_{th} iG-CLC system.

3.1 Carbon stripper

The carbon stripper separates the unconverted char particles from the oxygen carrier according to their different fluid dynamic properties. Char particles can be elutriated from the carbon stripper and recirculated to the fuel reactor using an appropriate fluidization flow [8], whereas the oxygen carrier particles are left to pass to the air reactor via the loop seal (2); see Figure 3. The separation efficiency of char from oxygen carrier is determined by the size distribution and density of both kinds of particles, which is related to their terminal velocity [43]. In fact, an efficient separation was reached with small coal particle size ($d_{p,av}$ = 47 μm) using a gas velocity in the carbon stripper around 0.25 m/s [8]; a separation efficiency above 99% was estimated [28]. Recently, a maximum separation has been observed in a 50 kW_{th} CLC unit when the gas velocity in the carbon stripper was in the 0.5-0.7 m/s interval with a higher particle size of coal ($d_{p,av}$ = 170 μm) [44]. In this work, considering terminal velocity for char particles ($u_{t,char}$ = 0.1 m/s) and oxygen carrier particles ($u_{t,OC}$ = 1 m/s), a gas velocity in the carbon stripper was assumed to be 0.65 m/s for a sharp separation, as proposed by Kramp et al. [43], and an acceptable carbon stripper efficiency of 98% was assumed. Thus, the carbon stripper operates in the bubbling fluidization regime; see Figure 5.

There has not yet been a study optimizing the design of a carbon stripper to minimize the cross sectional area, while maintaining high carbon separation efficiency. Here, the mass ratio between the gas to carbon stripper and the coal flow to the fuel reactor was fixed to be similar to that used in 100 kW_{th} and 1 MW_{th} CLC units [8,9]. Thus, the gas flow to the carbon stripper was taken to be 4.2 Nm^3/s. Under these assumptions a cross sectional area of 30 m^2 was calculated to operate at 0.65 m/s. The pressure drop in the carbon stripper was selected to be 15 kPa, but the gauge pressure at the carbon stripper must also account for part of the pressure drop in the fuel reactor. Considering the inlet point of solids entrained from the carbon stripper returning to the fuel reactor, the additional pressure drop to be overcome in the fuel reactor is 20 kPa; see Figure 3. With these conditions, a solids inventory in the carbon

stripper of 46000 kg was calculated. However, this amount could be lower if an optimized carbon stripper was designed. The main dimensions of the carbon stripper are shown in Table 1.

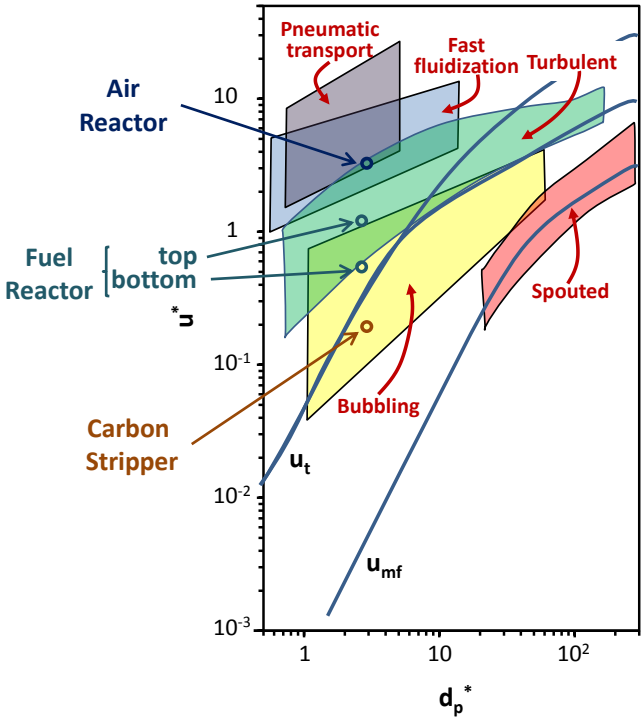

Figure 5. Fluidization regime for fuel reactor, air reactor and carbon stripper in the flow regime map [45]. $u^* = Re/Ar^{1/3}$; $d_p^* = Ar^{1/3}$.

3.2 Fuel reactor

Key parameters were identified in previous works to optimize the fuel reactor performance [2,28-30], the most relevant being the fuel reactor temperature, the amount of solids in the fuel reactor, and the oxygen carrier to fuel ratio. Figures 6(a-d) show, for the fuel reactor, the relation between its cross sectional area and other design parameters and operating conditions. Main dimensions of the fuel reactor are shown in Table 1. In the following, the reasons for the determination of several of these parameters are given:

- A temperature of 1000 ºC was suggested in the fuel reactor in order to improve the coal conversion in the fuel reactor and, hence, maximize the CO_2 capture [30].

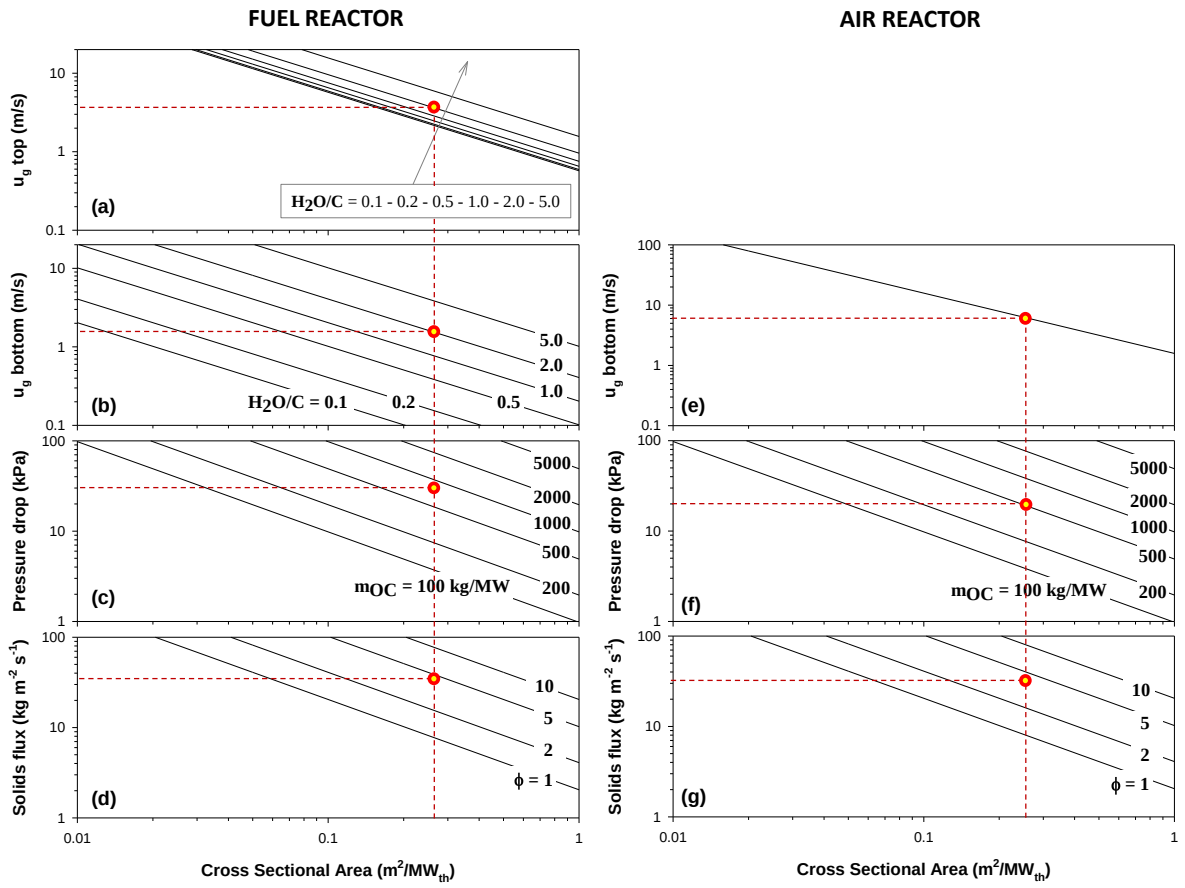

Figure 6. Relation between operating conditions and design parameters (steam to carbon molar ratio vs. gas velocity; solids inventory vs. pressure drop; oxygen carrier to fuel ratio, ϕ, vs. solids flux) as a function of the cross sectional area in the fuel and air reactors. Gas flow to the carbon stripper: 0.042 Nm^3/s per MW_{th}. Oxygen carrier: Ilmenite (R_{OC} = 4 wt.%). Symbol ⭘ shows design conditions.

- The cross sectional area of the fuel reactor is mainly defined by the desired gas velocity at the top and bottom of the reactor, as well as the steam to carbon ratio used; see Figures 6(a-b). Thus, the gas velocity can be increased by either increasing H_2O/C or decreasing the cross section. In *i*G-CLC, it is possible to operate with H_2O/C ratios lower than 1 due to H_2O is regenerated by reaction of H_2 with oxygen carrier [31]. However, very low H_2O/C ratios seems to be unpractical because of the related decrease in the cross sectional area and increase in the pressure drop to maintain constant the gas velocity and the solids

inventory; see Figures 6(b) and 6(c) together. In addition, low H_2O/C ratios can produce and inefficient generation of volatile matter with formation of solid carbon [46], i.e. a higher yield of fixed carbon which must be gasified. It is worth noting that the gas velocity in the upper part of the reactor is higher than in the bottom (Figure 6(a)) mainly due to the addition of gas coming from the carbon stripper and gas generated during coal conversion, i.e. volatile matter, gasification products and oxidized compounds by oxygen carrier; see Equations (1-4). The gas velocity is a relevant parameter to allow operating in the desired fluidization regime; see Figure 5. In this study, the fuel reactor assumed to be a turbulent fluidized bed, so as to be able to entrain the solids flux required for the selected oxygen carrier to fuel ratio (ϕ). For this design, the selected values for these gas velocities were 1.6 and 4 m/s at the inlet and outlet, respectively. With these design conditions, the gas flow fed to the fuel reactor is 8.7 Nm^3/s. Once the gas velocity was fixed, the cross sectional area and H_2O/C ratio was calculated by using Figures 6(a) and 6(b). A value of the steam to carbon molar ratio of $H_2O/C = 2$ and the cross sectional area of 25 m^2 was determined in order to avoid an excessive pressure drop in the fuel reactor; see Figure 6(c) for the solids inventory determined in the next point. Thus, the steam to fixed carbon molar ratio for design conditions is relatively high because of fluid dynamics requirements.

- Once the cross sectional area has been set, simulations were done with the theoretical model to evaluate the effect of the amount of solids in the fuel reactor on the performance of the process. Initially, a low oxygen carrier to fuel ratio (ϕ=1.5) was assumed in order to maximize the CO_2 capture rate [31]. Figure 7(a) shows the predicted values of CO_2 capture, η_{CC}, and total oxygen demand, Ω_T, as a function of the solids inventory. The CO_2 capture increased with the solids inventory, but it was high in all cases due to the presence of the carbon stripper (η_{CS} = 98% was assumed). A relevant effect on the total oxygen demand was predicted, mainly for solids inventory values lower than 750 kg/MW_{th}. However, increasing the solids inventory above 1000 kg/MW_{th} is not recommended

because the increase in the reactor size and/or pressure drop could not be justified by the low improvement of the combustion efficiency in the CLC unit. Considering the trade-off between solids inventory and improvement on the oxygen demand, a solids inventory of 750 kg/MW_{th} was considered in this work. Similar values were proposed in previous works [28,30]. However, the exact numbers of oxygen demand can vary for the same solids inventory when it was moving on a line in Figure 6(c), i.e. when both the pressure drop and the cross sectional area are changed, due to the different fluid dynamics. According to Figure 6(c), the corresponding pressure drop in the fuel reactor should be 30 kPa.

- For stoichiometric conditions (ϕ = 1), the required solids flux is 8.2 kg m^{-2} s^{-1}. However, lower oxygen demand values can be obtained by increasing the ϕ number; see Figure 7(b). Here an oxygen carrier to fuel ratio ϕ = 4 was assumed in order to maximize the combustion efficiency in the fuel reactor but still maintaining the CO_2 capture above 95% [28,30]. At assumption the corresponding solids flux increases to 32.7 kg m^{-2} s^{-1}; see Figure 6(d).

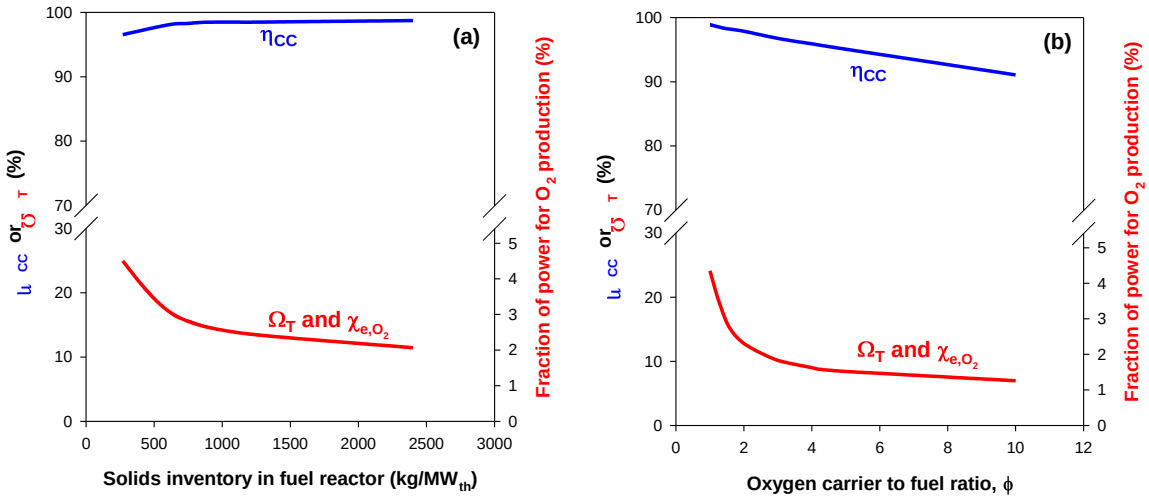

Figure 7. CO_2 capture, η_{CC}, total oxygen demand, Ω_T, and fraction of energy required to produce oxygen for the oxygen polishing as a function of (a) the solids inventory in the fuel reactor (ϕ=1.5); and (b) the oxygen carrier to fuel ratio (m_{FR}=750 kg/MW_{th}), ϕ. Predictions assuming η_{CS} = 98%.

Submitted, accepted and published by
Applied Energy, 2015, 157, 462-474

Table 1. Geometrical parameters and operational conditions of the fuel reactor, carbon stripper and air reactor (100 MW_{th}).

Reactor geometry	**Fuel reactor**	**Carbon stripper**	**Air reactor**
Height (m)	20	2	32
Cross section (m^2)	25	30	25
Height of the solid fuel feeding point (m)	0.1		
Height of inlet from carbon stripper (m)	0.7		
Height of dense phase (m)	1.5	1.1	-
Operational conditions			
Nominal thermal power (MW)	100		
Fuel flow (kg/s)	4.5		
Temperature (ºC)	1000	1000	1045
Total pressure drop (kPa)	30	15	20
Pressure drop from carbon stripper connection (kPa)	20		
Solids inventory (kg)	75000[a]	46000[b]	50000[c]
Inlet gas flow from distributor plate (Nm^3/s)	8.7[d]	4.2[e]	32.7
Exit gas flow (Nm^3/s)	20.6	4.3	27.8
Gas velocity at the bottom (m/s)	1.6	0.65	6
Gas velocity at the upper part (m/s)	4.0		
Solids circulation rate (kg/s)	820		
Oxygen carrier to fuel ratio	4		

[a] It could be lower with more reactive oxygen carriers
[b] Solids inventory in carbon stripper is not optimized
[c] Determined by pressure balance in the *i*G-CLC unit; the minimum solids inventory is 150 kg/MW_{th} (eq. 9)
[d] Steam
[e] CO_2

The total oxygen demand showed in Figures 7(a) and 7(b) are related to the flow of oxygen required in an oxygen polishing step downstream the fuel reactor to get complete combustion. Assuming a power consumption of P_{O_2} = 0.9 MW_e per kg/s of oxygen and a net plant efficiency of η_e = 41.6% [24], the fractional power to produce the oxygen can be estimated by:

$$\chi_{e,O_2} = \frac{10^3 P_{O_2} \Omega_T \Omega_{SF}}{\eta_e \left[\mathrm{LHV}\right]} \tag{10}$$

Thus, the power fraction of the CLC plant consumed in the oxygen production is relatively low for high solids inventory and high oxygen carrier to fuel ratio. Moreover, it is worth noting that the total oxygen demand, and hence the fraction of energy required to produce oxygen for the oxygen polishing, would be lower if more reactive oxygen carrier materials were used [30], e.g. Fe-ESF [15], Fe-ores [12] or Mn-ores [47].

3.3 Air reactor

In the air reactor the oxygen carrier is regenerated with air. Also, some char particles reach the air reactor if the carbon separation efficiency is lower than 100%. The carbon in these char particles is oxidized to CO_2, which is not captured. The air flow was set to be 20% in excess of that needed to burn the fuel fed to the fuel reactor, 32.7 Nm^3/s. For design purposes, Figures 6(e-g) show, for the air reactor, the relation between its cross sectional area and other design parameters and operating conditions. Thus, a high velocity ($u_{g,AR}$ = 6 m/s) is chosen, by reducing the cross sectional area of the reactor and to allow a high solids entrainment rate in the fast fluidization regime; see Figure 5. Accordingly, the air reactor cross sectional area was 25 m^2, see Figure 6(e), equal to the fuel reactor. The required solids flux is 32 kg m^{-2} s^{-1}, see Figure 6(g), which may be easily reached under these conditions. If a higher solids flux was reached, a fraction of the exit solids stream should be recirculated to the air reactor to fit the desirable solids circulation rate, in a similar way that proposed in [16]. The pressure drop in

the air reactor was set to 20 kPa in order to insure the proper operation of the loop seal (2); see Figure 3. With these assumptions the solids inventory was around 500 kg/MW_{th}, as is shown in Figure 6(f). The main dimensions of the air reactor are shown in Table 1. The determination of the air reactor height is described in Section 3.4.

Nevertheless, considering the reactivity of activated ilmenite particles, the minimum solids inventory in the air reactor was estimated to be 150 kg/MW_{th} by using equation (9). Therefore, there is a possibility to reduce the solids inventory in the air reactor if the loop seal (2) could be operated properly, for example by controlling the pressure of the air reactor itself. The air reactor temperature depends on the enthalpy balance.

3.4 Cyclones system

Solids entrained from the reactors are separated by a cyclone system and sent to the next element in the *i*G-CLC unit. The dimensioning of the cyclone is based on a high efficiency standard cyclone, with a gas velocity at the cyclone inlet of 15 m/s [48]. A system of four cyclones was assumed in both air and fuel reactor; see Figure 4. The dimensions of the cyclones are shown in Table 2. The size of cyclones must be considered to evaluate the over-all height of the air and fuel reactors in the arrangement of all the elements of the *i*G-CLC unit. Thus, if the required solids in the air reactor determined a reactor height lower than the cyclone height, the cyclone height will determine the air reactor height. The air reactor height is 32 m, whereas the fuel reactor is 20 m tall. Peltola et al. [22] determined that the air reactor height should be 25 m in order to include membrane walls to extract the required heat in a 100 MW_{th} CLC unit. Thus, the air reactor height determined for cyclone arrangement was higher than that required to extract heat.

Table 2. Dimensions for the cyclones of a 100 MW_{th} *i*G-CLC system [48].

Submitted, accepted and published by
Applied Energy, 2015, 157, 462-474

	Fuel reactor	Air reactor
H_C (m)	2.0	2.3
B_C (m)	0.8	0.9
D_C (m)	4.0	4.7
L_C (m)	6.0	7.0
Z_C (m)	9.9	11.7
J_C (m)	1.5	1.8
D_e (m)	2.0	2.3

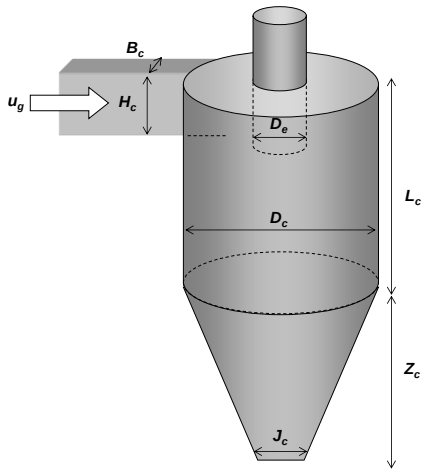

3.5 Loops seal system

Loop seals prevent the mixing of gases between different elements in the *i*G-CLC unit. Thus, a loop seal must balance the pressure between the elements it connects. The length of the low pressure side of each loop seal is given by the pressure balance in the system, as is shown in Figure 3. Thus, loop seal (1) is necessary to avoid the malfunction of the cyclones on the fuel reactor due to the leaking of gas from the carbon stripper to these cyclones. It must balance an overpressure of 20 kPa due to the distance between the fuel reactor inlet point from the carbon stripper and the fuel reactor cyclone exit. Loop seal (2) prevents the mixing of air from the air reactor and CO_2 in the carbon stripper. It must balance a low pressure difference between the air reactor and the upper part of the carbon stripper. Loop seal (3) hinders the mixing of air from the air reactor and gases in the fuel reactor. Loop seal (3) must be carefully designed since it must balance a high pressure difference between the air reactor cyclone and the bottom part of the fuel reactor, in this case 30 kPa. Thus, the length of the low pressure side of each loop seal is given by the pressure balance in the system, and it must be at least 1.6 and 2.4 m for loop seals (1) and (3), respectively.

Also, the loop seal units must be large enough to allow a high solids circulation flow rate, i.e. the loop seal must no limit the solids circulation flow rate. Commonly, loop seals allow a solids flow of 300 kg m^{-2} s^{-1} [49], which will define its cross section.

4 Performance of the 100 MW_{th} *i*G-CLC unit

The performance of the fuel reactor was measured in terms of the CO_2 capture efficiency, η_{CC}, and the total oxygen demand, Ω_T, as predicted by the theoretical model. Both parameters are relevant for the subsequent mass and enthalpy balances to the *i*G-CLC unit. Clearly, the CO_2 capture rate depends strongly on the efficiency of the carbon stripper separating char from oxygen carrier particles, η_{CS} [29]. Thus, a value of the CO_2 capture of η_{CC} = 50.5 % is predicted by the model when a carbon separation system is not considered, i.e. η_{CS} = 0. The absence of a carbon stripper gives low CO_2 capture values because of the low char conversion in the fuel reactor, calculated to be X_{char} = 36%. But a CO_2 capture rate higher than 95% is predicted when a highly efficient carbon stripper ($\eta_{CS} \geq$ 98%) is included in the *i*G-CLC scheme.

There is an energy penalty in the process due to the use of steam as the gasifying agent fed to the fuel reactor [36]. Thus, the use of CO_2 from the recirculated flue gases could be beneficial, as it would reduce the energy needs related to steam generation. This is practical in this case for sub-bituminous Tremedal coal because the CO_2 gasification rate is higher than H_2O gasification rate; see Supplementary Information. Thus, the use of CO_2 as fluidization medium could be advantageous when sub-bituminous coals were used as fuel. Figure 8 shows the CO_2 capture efficiency and total oxygen demand in the fuel reactor for a range of steam and CO_2 mixtures as predicted by the model assuming four different values for the carbon stripper efficiency, η_{CS}. Both the CO_2 capture and total oxygen demand increased with the increase of the efficiency of the carbon stripper; but they are barely influenced by the

composition of the gasification agent. For evaluation purposes, a carbon separation efficiency of η_{CC} = 98% will be assumed. A similar value for η_{CS} has been calculated for a carbon stripper included in a 100 kW_{th} CLC unit [28]. At this condition, the value of Ω_T only decreased from 8.6 to 7.1% when H_2O was replaced by CO_2. The corresponding oxygen flow in the oxygen polishing unit would be 0.71-0.58 kgO_2/s. Assuming a power consumption of 0.9 MW_e per kg/s of oxygen and a net plant efficiency of 41.6% [24], a power of 0.64-0.52 MW_e for the oxygen production in the 41.6 MW_e CLC unit (100 MW_{th}) was calculated, i.e. a decrease of χ_{e,O_2} = 1.5-1.25% in the net plant efficiency; see equation (10).

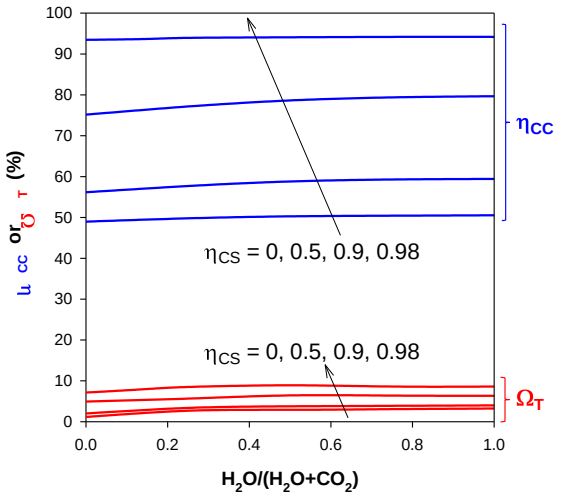

Figure 8. CO_2 capture (η_{CC}) and total oxygen demand (Ω_T) predicted in the 100 MW_{th} *i*G-CLC unit for varying H_2O and CO_2 mixtures as fluidizing agent in the fuel reactor, assuming various carbon separation efficiencies, η_{CS}.

In order to evaluate the performance of the whole *i*G-CLC unit, both fuel and air reactor models were coupled and solved jointly. It was determined that the oxygen carrier must be highly oxidized in the air reactor. This was calculated to be $X_{OC,AR}$ = 0.8 in order to fit the variation in oxygen carrier conversion $\Delta X_{OC} = (1-\Omega_T)*(X_{OC,AR}-X_{OC,FR})$ = 0.23. Table 3 shows the gas composition predicted by the model at the fuel reactor exit when steam or CO_2 was

used as fluidizing agent, and assuming η_{CS} = 98%. Gases exiting the cyclone system must be addressed before the CO_2 purification and compression units, especially with regard to unburned fuel and sulphur compounds. Their complete combustion, using a pure oxygen polishing step, is considered in this work when calculating the mass and enthalpy balances for the *i*G-CLC system, although different options have been considered in the literature [2].

Table 3. Flow rates and composition of gases exiting the fuel and air reactors, predicted with the model for η_{CS} = 98%, and solids inventory of 750 and 500 kg/MW_{th} in fuel and air reactors, respectively.

Fluidizing agent	H_2O		CO_2	
Fuel reactor	Flow rate (Nm^3/s)	vol. %	Flow rate (Nm^3/s)	vol. %
H_2O	11.69	57.4	3.16	15.4
CO_2	7.88	38.7	16.53	80.4
CO	0.29	1.4	0.44	2.1
H_2	0.22	1.1	0.21	1.0
CH_4	0.10	0.5	0.031	0.2
SO_2	0.15	0.7	0.16	0.8
H_2S	0.022	0.1	0.013	0.1
N_2	0.016	0.1	0.016	0.1
Air reactor	Flow rate (Nm^3/s)	vol. %	Flow rate (Nm^3/s)	vol. %
N_2	26.50	93.2	26.50	93.3
O_2	1.65	5.8	1.63	5.8
CO_2	0.25	1.0	0.22	0.9

Submitted, accepted and published by
Applied Energy, 2015, 157, 462-474

5 Evaluation of the *i*G-CLC process

From the results of this study, the performance of the *i*G-CLC process burning Tremedal coal has some benefits using CO_2 as fluidizing gas rather than using steam. Moreover, the thermal integration of the *i*G-CLC process with the steam cycle and steam generation will be influenced by using either steam or CO_2. The simplified Sankey diagrams in Figure 9 show the enthalpy flow in the *i*G-CLC system for steam or CO_2 fluidization. In the enthalpy balance it was assumed that the initial temperature of the air, liquid water and CO_2 was 25 ºC, and they were pre-heated to 400 ºC before entering the air reactor, fuel reactor, carbon stripper or loop seals. The thermal input was 100 MW_{th} based on the LHV of the coal.

Firstly, it is important to remember that the air reactor must be partially cooled in order to control its temperature. Heat exchangers must be designed considering the heat flux required in each case. The extracted heat flux that must be accommodated in the air reactor was lower when CO_2 was used as fluidizing gas because of the higher heat capacity of the gases from fuel reactor when CO_2 was used. Thus, a higher fraction of sensible heat in gases from fuel reactor was related to a lower heat flow extracted from the air reactor, in order to fulfil the global enthalpy balance.

In addition, the fraction of the thermal input (100 MW_{th} based on LHV) required to pre-heat the inlet gas stream to fuel reactor is higher for the steam gasification option, i.e. 21.3 vs. 6.1 MW_{th}; see Figures 9(a) and 9(b). Also, the low level heat in steam from the fuel reactor is significantly reduced. Eventually, the difference in the steam flow at the fuel reactor exit will give higher net plat efficiency when CO_2 is used. In this sense, Fillman et al. [36] calculated a net plant efficiency of 41% when H_2O was used, and increased to 42% when H_2O was replaced by recirculated CO_2.

The output power is recovered from the air reactor and hot gaseous exit streams. Only a small amount of power can be recovered from the hot fly ash. To analyze the available output power in each mode, the recovered sensible heat, RSH, is defined from the Sankey diagrams as:

Submitted, accepted and published by
Applied Energy, 2015, 157, 462-474

$$\mathrm{RSH} = \frac{1}{P_{th}}\left\{\left[\sum_i \int_{298K}^{T_{in}} \dot{m}_i c_{p,i}\mathrm{d}T\right]_{\text{out streams}} + Q_{ext,AR} - \left[\dot{m}_{H_2O}\lambda_{H_2O} + \sum_i \int_{298K}^{673K} \dot{m}_i c_{p,i}\mathrm{d}T\right]_{\text{in streams}}\right\} \quad (11)$$

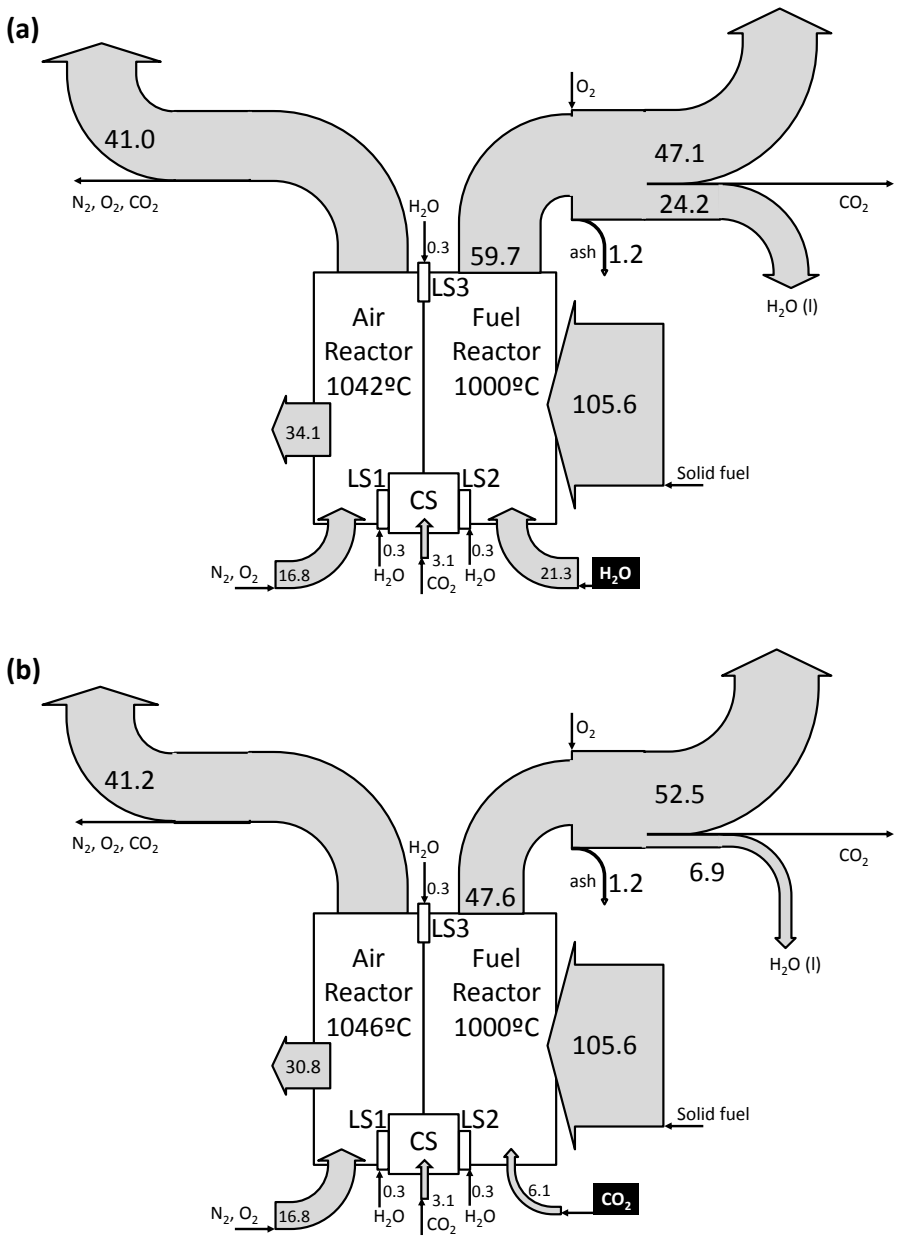

Figure 9. Simplified Sankey diagram with the enthalpy flows to and from the *i*G-CLC system with the fluidization agent (a) H_2O or (b) CO_2. All numbers are given in thermal MW. Input fuel power was calculated considering the higher heating value of Tremedal coal (HHV =23230 kJ/kg).

RSH represents the enthalpy in outlet streams, both sensible heat and heat extracted from the air reactor, minus the total heat used in evaporating steam and pre-heating gases in the inlet

streams. Thus, heat from steam condensation is not considered as useful energy. The use of steam as the fluidizing gas has an important penalty in the RSH, which is 81.4%, when steam is used compared to 98.7% when CO_2 is used. Thus, for several reasons, the use of CO_2 in the fuel reactor is advantageous over the use of steam. In either case, high CO_2 capture rates could be obtained in coal combustion by *i*G-CLC. It is worth noting that the solid fuel chosen for this work was a high reactive coal, with a high gasification rate with CO_2. For low reactive coals, the carbon stripper efficiency should be higher in order to reach similar values of CO_2 capture rates.

6 Conclusions

The basic design of a 100 MW_{th} *i*G-CLC unit for coal combustion has been presented. Ilmenite was considered to be the oxygen carrier, and a highly reactive sub-bituminous coal was the fuel. The solids inventory in the fuel reactor was determined to be 750 kg/MW_{th}, and the oxygen carrier to fuel ratio was $\phi = 4$. Fluid dynamic considerations and cyclone sizes affected the design of the complete CLC loop, including the height and section of the fuel reactor, carbon stripper, air reactor and loop seals. Simulations indicated the benefits of decreasing the steam flow to the fuel reactor, which must be replaced by recycled CO_2 to maintain the fuel reactor in the high-velocity fluidized bed mode. Slightly higher CO_2 capture and lower oxygen demand was obtained when CO_2 was used as fluidizing gas in the fuel reactor instead of steam because of the higher reactivity of Tremedal coal to CO_2 gasification. Thus, 7% of oxygen demand and 95% CO_2 capture were predicted. Moreover, more important were the benefits of using CO_2 on the integration of *i*G-CLC based power plant.

Acknowledgment

Submitted, accepted and published by
Applied Energy, 2015, 157, 462-474

This work was supported by Shell Global Solutions International BV (Contract PT26961).

Nomenclature

$c_{p,i}$	heat capacity (J kg^{-1} K^{-1})
$d_{p,av}$	average particle diameter (m)
F_i	molar flow of specie *i* (mol/s)
g	gravity acceleration (9.8 m/s^2)
$\dot{H}_i$	enthalpy flux of specie *i* (J/s)
m_{OC}	mass of oxygen carrier (kg)
$\dot{m}_i$	mass flow of specie *i* (kg/s)
P_{O_2}	power consumption to generate oxygen for the oxygen polishing (MW_e per kg/s of oxygen)
P_{th}	thermal power of the CLC unit (MW_{th})
Q_i	heat flux of specie *i* (J/s)
R_{OC}	oxygen transport capacity (kgO/kgOC)
t	time (s)
T	temperature (K)
u_g	gas velocity of particles (m/s)
u_t	terminal velocity of particles (m/s)
X_{char}	char conversion
X_{OC}	oxygen carrier conversion

Greek letters

χ_{e,O_2} fractional power to produce the oxygen for the oxygen polishing

ΔX_{OC} difference of the oxygen carrier conversion between air and fuel reactors

ϕ oxygen carrier to fuel ratio

λ_{H_2O} vaporization latent heat (J/kg)

η_{CC} carbon dioxide capture efficiency

η_{CS} carbon stripper efficiency

η_e net plant efficiency (MW_e/MW_{th})

μ_g gas viscosity (kg m^{-1} s^{-1})

ρ_g gas density (kg/m^3)

ρ_p particle density (kg/m^3)

ξ_{g-s} gas-solid contact efficiency

Ω_{SF} oxygen demanded by the solid fuel (kgO/kgSF)

Ω_T total oxygen demand

Dimensionless groups

Ar Archimedes number ($d_{p,av}^3 \rho_g(\rho_p-\rho_g)g/\mu_g^2$)

Re Reynolds number ($u_g \rho_g d_{p,av}/\mu_g$)

Subscripts

AR air reactor

CS carbon stripper

ext extracted

FR fuel reactor

g gas

in inlet

LS loop seal

O oxygen

OC oxygen carrier

out outlet

prod products

reac reactants

SC steam condensation

SF solid fuel

Acronims

HHV Higher Heating Value (kJ/kg)

*i*G-CLC *in-situ* Gasification Chemical Looping Combustion

LHV Lower Heating Value (kJ/kg)

RSH Recovered Sensible Heat

References

[1] Adanez, J., Abad, A., García-Labiano, F., Gayán, P., de Diego, L.F. (2012), Progress in Chemical-Looping Combustion and Reforming technologies, *Progress in Energy and Combustion Science* **38**, pp. 215-282.

[2] Gayán, P., Abad, A., de Diego, L.F., García-Labiano, F., Adánez, J. (2013), Assessment of technological solutions for improving chemical looping combustion of solid fuels with CO_2 capture, *Chemical Engineering Journal* **233**, pp. 56-69.

[3] Mendiara, T., Izquierdo, M.T., Abad, A., de Diego, L.F., García-Labiano, F., Gayán, P., Adánez, J. (2014), Release of pollutant components in CLC of lignite, *International Journal of Greenhouse Gas Control* **22**, pp. 15-24.

[4] Adánez-Rubio, I., Abad, A., Gayán, P., García-Labiano, F., de Diego, L.F., Adánez, J. (2014), The fate of sulphur in the Cu-based Chemical Looping with Oxygen Uncoupling (CLOU) Process, *Applied Energy* **113**, pp. 1855-1862.

[5] Lyngfelt, A. (2014), Chemical-looping combustion of solid fuels - Status of development, *Applied Energy* **113**, 1869-1873.

[6] Berguerand, N., Lyngfelt, A. (2008), Design and operation of a 10 kWth chemical-looping combustor for solid fuels - Testing with South African coal, *Fuel* **87**, pp. 2713-2726.

[7] Cuadrat, A., Abad, A., García-Labiano, F., Gayán, P., de Diego, L.F., Adánez, J. (2011), The use of ilmenite as oxygen-carrier in a 500 Wth Chemical-Looping Coal Combustion unit, *International Journal of Greenhouse Gas Control* **5**, pp. 1630-1642.

[8] Markström, P., Linderholm, C., Lyngfelt, A. (2013), Chemical-looping combustion of solid fuels - Design and operation of a 100 kW unit with bituminous coal, *International Journal of Greenhouse Gas Control* **15**, pp. 150-162.

[9] Ströhle, J., Orth, M., Epple, B. (2014), Design and operation of a 1 MW_{th} chemical looping plant, *Applied Energy* **113**, pp. 1490-1495.

[10] Abad, A., Pérez-Vega, R., de Diego, L.F., García-Labiano, F., Gayán, P., Adánez, J. (2015), Design and operation of a 50 kW_{th} Chemical Looping Combustion (CLC) unit for solid fuels, *Applied Energy*, submitted.

[11] Thon, A., Kramp, M., Hartge, E.-U., Heinrich, S., Werther, J. (2014), Operational experience with a system of coupled fluidized beds for chemical looping combustion of solid fuels using ilmenite as oxygen carrier, *Applied Energy* **118**, pp. 309-317.

[12] Mendiara, T., de Diego, L.F., García-Labiano, F., Gayán, P., Abad, A., Adánez, J. (2014), On the use of a highly reactive iron ore in Chemical Looping Combustion of different coals, *Fuel* **126**, pp. 239-249.

[13] Song, T., Shen, T., Shen, L., Xiao, J., Gu, H., Zhang, S. (2013), Evaluation of hematite oxygen carrier in chemical-looping combustion of coal, *Fuel* **104**, pp. 244-252.

[14] Andrus, H., Chui, J., Thibeault, P., Edberg, C., Turek, D., Kenney, J., Abdulally, I., Chapman, P., Kang, S., Lani, B. (2012), Alstom's limestone-based (LCL^{TM}) chemical looping process, *Proceeding from the 2nd International Conference on Chemical Looping*, Darmstadt, Germany.

[15] Mendiara, T., de Diego, L.F., García-Labiano, F., Gayán, P., Abad, A., Adánez, J. (2013), Behaviour of a bauxite waste material as oxygen carrier in a 500 Wth CLC unit with coal, *International Journal of Greenhouse Gas Control* **17**, pp. 170-182.

[16] Morin, J.-X., Béal, C. (2005), Chemical Looping Combustion of refinery fuel gas with CO_2 capture, *Chapter 37 in Carbon Dioxide Capture for Storage in Deep Geologic Formations, Volume 1*, D.C. Thomas and S.M. Benson (Eds.).

[17] Naqvi, R., Bolland, O., Wolf, J. (2005), Off-design evaluation of a natural gas fired Chemical Looping Combustion Combined Cicle with CO_2 capture, *Proceeding from ECOS 2005*, Trondheim, Norway.

[18] Wolf. J., Anheden, M., Yan, J. (2005), Comparison of nickel- and iron-based oxygen carrier in chemical looping combustion for CO2 capture in power generation, *Fuel* **84**, pp. 993-1006.

[19] Kramp, M., Thon, A., Hartge, E.-U., Heinrich, S., Werther, J. (2011), Challenges with the coupling of fluidized beds for Chemical Looping Combustion, *Proceedings from the 13th International Conference on Fluidization – New Paradigm in Fluidization Engineering*, Gyeong-ju, Korea, May 16-21, 2010.

[20] Sharma, R., Chandel, M.K., Delebarre, A., Alappat, B. (2013), 200-MW chemical looping combustion based thermal power plant for clean power generation, *International Journal of Energy Research* **37**, pp. 49-58.

[21] Marx, K., Pröll, T., Hofbauer, H. (2012), Next scale Chemical Looping Combustion: fluidized bed system design for demonstration unit, *Proceedings from the 21th International Conference on Fluidized Bed Combustion*, Naples, Italy.

[22] Peltola, P., Ritvanen, J., Tynjälä, T., Hyppänen, T. (2013), Model-based evaluation of a chemical looping combustion plant for energy generation at a pre-commercial scale of 100 MW_{th}, *Energy Conversion and Management* **76**, pp. 323-331.

[23] Schöny, G., Pallarès, D., Leion, H., Wolf, J. (2011), Assessment of the Scale-Up and Operational Design of the Fuel Reactor in Chemical Looping Combustion, *Proceedings of the 36th International Technical Conference on Clean Coal & Fuel Systems*, Clearwater, Florida, USA.

[24] Authier, O., Le Moullec, Y. (2013), Coal Chemical-Looping Combustion for Electricity Generation: Investigation for a 250 MW_e Power Plant, *Energy Procedia* **37**, pp. 588-597.

[25] Peltola, P., Ritvanen, J., Tynjälä, T., Hyppänen, T. (2015), Fuel reactor modelling in chemical looping with oxygen uncoupling process, *Fuel* **147**, pp. 184-194.

[26] Penthor, S., Zerobin, F., Mayer, K., Pröll, T., Hofbauer, H. (2015), Investigation of the performance of a copper based oxygen carrier for chemical looping combustion in a 120 kW pilot plant for gaseous fuels, *Applied Energy* **145**, pp. 52-59.

[27] Abad, A., Gayán, P., García-Labiano, F., de Diego, L.F., Adánez, J. (2014), Relevance of Oxygen Carrier Characteristics on CLC Design for Gaseous Fuels, *Poster presented at 3rd International Conference on Chemical Looping*, Gothenburg, Sweden.

[28] Abad, A., Adánez, J., de Diego, L.F., Gayán, P., García-Labiano, F., Lynfelt, A. (2013), Fuel reactor model validation: Assessment of the key parameters affecting the chemical-looping combustion of coal, *International Journal of Greenhouse Gas Control* **19**, pp. 541-551.

[29] Abad, A., Gayán, P., de Diego, L.F., García-Labiano, F., Adánez, J. (2013), Fuel reactor modelling in chemical-looping combustion of coal: 1. model formulation, *Chemical Engineering Science* **87**, pp. 277-293.

[30] García-Labiano, F., de Diego, L.F., Gayán, P., Abad, A., Adánez, J. (2013), Fuel reactor modelling in chemical-looping combustion of coal: 2-Simulation and optimization, *Chemical Engineering Science* **87**, pp. 173-182.

[31] Cuadrat, A., Abad, A., García-Labiano, F., Gayán, P., de Diego, L.F., Adánez, J. (2012), Effect of operating conditions in Chemical-Looping Combustion of coal in a 500 W_{th} unit, *International Journal of Greenhouse Gas Control* **6**, pp. 153-163.

[32] Cuadrat, A., Abad, A., García-Labiano, F., Gayán, P., de Diego, L.F., Adánez, J. (2012), Relevance of the coal rank on the performance of the in situ gasification chemical-looping combustion, *Chemical Engineering Journal* **195-196** , pp. 91-102.

[33] Cuadrat, A., Abad, A., de Diego, L.F., García-Labiano, F., Gayán, P., Adánez, J. (2012), Prompt considerations on the design of Chemical-Looping Combustion of coal from experimental tests, *Fuel* **97**, pp. 219-232.

[34] Cuadrat, A., Abad, A., Gayán, P., de Diego, L.F., García-Labiano, F., Adánez, J. (2012), Theoretical approach on the CLC performance with solid fuels: Optimizing the solids inventory, *Fuel* **97**, pp. 536-551.

[35] Mendiara, T., Abad, A., de Diego, L.F., García-Labiano, F., Gayán, P., Adánez, J. (2013), Biomass combustion in a CLC system using an iron ore as an oxygen carrier, *International Journal of Greenhouse Gas Control* **19**, pp. 322-330.

[36] Fillman, B., Anheden, M., Wolf, J. (2009), Parameter study in order to reveal critical design issues in the design for a CLC power plant using solid carbon as fuel, *Proceedings from the 1st International Conference on Chemical Looping*, Lyon, France.

[37] Abad, A., Adánez, J., Cuadrat, A., García-Labiano, F., Gayán, P., de Diego, L.F. (2011), Kinetics of redox reactions of ilmenite for chemical-looping combustion, *Chemical Engineering Science* **66**, pp. 689-702.

[38] Adánez, J., Cuadrat, A., Abad, A., Gayán, P., de Diego, L.F., García-Labiano, F. (2010), Ilmenite Activation during Consecutive Redox Cycles in Chemical-Looping Combustion, *Energy Fuels* **24**, pp. 1402-1413.

[39] Cuadrat, A., Abad, A., Adánez, J., de Diego, L.F., García-Labiano, F., Gayán, P. (2010), Behavior of ilmenite as oxygen carrier in chemical-looping combustion, *Fuel Processing Technology* **94**, pp. 101-112.

[40] Pallarès, D., Johnsson, F. (2006), Macroscopic modelling of fluid dynamics in large-scale circulating fluidized beds, *Progress in Energy and Combustion Science* **32**, pp. 539-569.

[41] Abad, A., Adánez, J., García-Labiano, F., de Diego, L.F., Gayán, P. (2010), Modeling of the chemical-looping combustion of methane using a Cu-based oxygen-carrier, *Combustion Flame* **157**, pp. 602-615.

[42] Furusaki, S., Kikuchi, T., Miyauchi, T. (1976), Axial Distribution of Reactivity Inside a Fluid-Bed Contactor, *AIChE Journal* **22**, pp. 354-361.

[43] Kramp, M., Thon, A., Hartge, E.-U., Heinrich, S., Werther, J. (2012), Carbon Stripping – A Critical Process Step in Chemical Looping Combustion of Solid Fuels, *Chemical Engineering Technology* **35**, pp. 497-507.

[44] Pérez-Vega, R. Abad, A., de Diego, L.F., García-Labiano, F., Gayán, P., Adánez, J. (2015), Coal Combustion with CO_2 Capture in a 50 kW_{th} Chemical Looping Combustion Unit, *7th International Conference on Clean Coal Technologies (CCT2015)*, Krakow, Poland.

[45] Kunii, D., Levenspiel, O. (1997), Circulating fluidized-bed reactors, *Chemical Engineering Science* **52**, pp. 2471-2482.

[46] Johnson, JL. (1981), Fundamentals of coal gasification. In: Elliot MA, editor. *Chemistry of coal utilization (second supplementary volume)*. 2nd ed. New York: John Wiley and Sons; p. 1491–598.

[47] Lyngfelt, A., Linderholm, C. (2014), Chemical-Looping Combustion of Solid Fuels - Technology Overview and Recent Operational Results in 100 kW Unit, *Energy Procedia* **63**, pp. 98-112.

[48] Sinnot, R.K. (1983), Chemical Engineering, Vol. 6, An Introduction to Chemical Engineering Design; *in Chemical Engineering* series by J.M. Coulson and J.F. Richardson; Pergamon Press; Oxford, England.

[49] Marx, K., Pröll, T., Hofbauer, H. (2012), Next scale chemical looping combustion: fludized bed system design for demonstration unit, *Proceeding from the 21st International Conference on Fluidized Bed Combustion*, Naples, Italy.